

Summation by parts operators for finite difference approximations of second-derivatives with variable coefficients

October 7, 2010

Abstract

Finite difference operators approximating second derivatives with variable coefficients and satisfying a summation-by-parts rule have been derived for the second-, fourth- and sixth-order case by using the symbolic mathematics software Maple. The operators are based on the same norms as the corresponding approximations of the first derivative, which makes the construction of stable approximations to general multi-dimensional hyperbolic-parabolic problems straightforward.

Key words: high-order finite difference methods, numerical stability, second-derivatives, variable coefficients

1 Introduction

In many applications, such as general relativity [28, 3], seismology [12, 30], oceanography [21], acoustics [29, 22, 5, 2, 6] and electromagnetics [31, 7], the underlying equations are systems of second-order hyperbolic partial differential equations. However, as pointed out in [13], with very few exceptions the equations are rewritten and solved as a system of first-order equations. There are some benefits by solving the equations on second-order form [16]. However, stability is not so easily shown for a narrow-stencil approximation of such problems. In [19] we introduced the term *narrow*, to define explicit finite difference schemes with a minimal stencil width.

Narrow-stencil approximations of second-derivatives have long been known to have good accuracy properties [19]. Narrow-stencil second-derivative

summation-by-parts (SBP) operators approximating $\partial^2/\partial x^2$ were derived in [17]. In this paper we derive narrow-stencil SBP operators approximating $\partial/\partial x (b(x) \partial/\partial x)$, where $b(x) > 0$. Stability for higher-order accurate (higher than third-order) narrow-stencil finite difference approximations applicable to second-order hyperbolic systems on general curvilinear grids have never before been fully addressed. The main reason has been the failure of deriving narrow-stencil higher-order accurate SBP operators for variable coefficient second-derivatives.

In [19] we introduced an important relationship between the existing first- and second-derivative SBP operators, referred to as *compatibility*. The main result of that study [19] was to prove that compatibility is a necessary condition obtaining an energy estimate (i.e., proving stability) for narrow-stencil approximations of problems with a combination of mixed ($\partial^2/\partial x \partial y$) and non-mixed ($\partial^2/\partial x^2, \partial^2/\partial y^2$) second-derivatives. However, that study was limited to the constant coefficient case. Typical applications deal with the corresponding variable coefficient case. Hence, problems with a combination of mixed $\partial/\partial x (b_{12}(x, y) \partial/\partial y)$, $\partial/\partial y (b_{21}(x, y) \partial/\partial x)$ and pure $\partial/\partial x (b_{11}(x, y) \partial/\partial x)$, $\partial/\partial y (b_{22}(x, y) \partial/\partial y)$ second-derivatives with variable coefficients, such as the compressible Navier-Stokes equations [20, 24, 25] and various second-order hyperbolic systems on curvilinear grids. The main result of the present study is the derivation and construction of narrow-stencil compatible SBP operators also for the variable coefficient problem. This is the first time such finite difference operators have been presented in literature. It is imperative to use finite difference approximations that do not allow growth in time—a property termed “strict stability” [9]. The combination of narrow-stencil SBP operators and the Simultaneous Approximation Term (SAT) method [4] to implement the boundary and interface conditions [15] makes it possible to exactly mimic the continuous energy estimate and thus proving strict stability. In a coming study we will make use of the newly derived SBP operators to obtain strictly stable wave propagation for complex 2-D and 3-D applications.

In Section 2 we introduce the SBP-SAT method for a 1-D second-order hyperbolic problem. A detailed construction procedure for the compatible SBP operators are presented in Section 3. In Section 4 we analyze a 2-D hyperbolic system on second-order form having both mixed and pure second-derivatives with variable coefficients. We show that compatibility is a necessary condition obtaining an energy estimate for narrow-stencil approximations of such problems. In section 5 the accuracy and stability properties of the newly developed SBP operators are verified by performing numerical simulations in 1-D. In Section 6 conclusions are drawn. The SBP operators are presented in Appendix I.

2 Definitions

The following definitions are needed in Section 4, to analyze the stability properties of the new SBP operators. Let the inner product for real-valued functions $u, v \in L^2[0, 1]$ be defined by $(u, v) = \int_0^1 u v a(x) dx$, $a(x) > 0$, and let the corresponding norm be $\|u\|_a^2 = (u, u)$. The domain $(0 \leq x \leq 1)$ is discretized using the following $N + 1$ equidistant grid points:

$$x_i = i h, \quad i = 0, 1, \dots, N, \quad h = \frac{1}{N}.$$

The approximate solution at grid point x_i is denoted v_i , and the discrete solution vector is $v^T = [v_0, v_1, \dots, v_N]$. Similarly, we define an inner product for discrete real-valued vector functions $u, v \in \mathbf{R}^{N+1}$ by $(u, v)_{H_a} = u^T H A v$, where H is diagonal and positive definite and A is the projection of $a(x)$ onto the diagonal. The corresponding norm is $\|v\|_{H_a}^2 = v^T H A v$.

Remark The matrix product HA defines a norm iff HA is symmetric and positive definite. This can only be guaranteed if H is a diagonal matrix (see [23] for a detailed study on this).

The following vectors will be frequently used:

$$e_0 = [1, 0, \dots, 0]^T, \quad e_N = [0, \dots, 0, 1]^T. \quad (1)$$

2.1 The SBP-SAT method

To define the SBP-SAT method, we present the following two definitions (first stated in [19]):

Definition 2.1 *An explicit p th-order accurate finite difference scheme with minimal stencil width of a Cauchy problem is called a p th-order accurate narrow-stencil.*

Definition 2.2 *A difference operator $D_1 = H^{-1}Q$ approximating $\partial/\partial x$, using a p th-order accurate narrow-stencil, is said to be a p th-order accurate narrow-diagonal first-derivative SBP operator if H is diagonal and positive definite and $Q + Q^T = \text{diag}(-1, 0, \dots, 0, 1)$.*

We say that a scheme is explicit if no linear system of equations needs to be solved to compute the difference approximation. Spatial Padé discretizations [14] are often referred to as “compact schemes.” The approximation of the derivative is obtained by solving a tri- or penta-diagonal system of linear equations at every time step. Hence, if written in explicit form, Padé discretizations lead to full-difference stencils, similar to spectral discretizations.

In the present study the focus is on deriving SBP operators for systems involving a combination of mixed and pure second-derivative terms with variable coefficients. As an example of the simple, yet powerful, SBP-SAT method, we consider the following second-order hyperbolic equation:

$$\begin{aligned} au_{tt} &= (bu_x)_x, & 0 \leq x \leq 1, & \quad t \geq 0, \\ \alpha u_t - bu_x &= g, & x = 0, & \quad t \geq 0, \\ \alpha u_t + bu_x &= g, & x = 1, & \quad t \geq 0, \end{aligned} \quad (2)$$

where $a(x) > 0$ and $b(x) > 0$. Multiplying the first equation in (2) by u_t , integrating by parts (referred to as “the energy method”) and imposing the boundary conditions leads to

$$\frac{d}{dt} (\|u_t\|_a + \|u_x\|_b) = -2(\alpha u_t - g)u_t|_{x=1} - 2(\alpha u_t - g)u_t|_{x=0}. \quad (3)$$

An energy estimate is obtained if $\alpha \geq 0$. The discrete approximation of (2) using the SBP-SAT method is

$$\begin{aligned} Av_{tt} &= D_1 B D_1 v - H^{-1} \tau e_0 \{(\alpha v_t - B D_1 v)_0 - g\} \\ &\quad - H^{-1} \tau e_N \{(\alpha v_t + B D_1 v)_N - g\}, \end{aligned} \quad (4)$$

where e_0 and e_N are defined in (1). The matrices A and B have the values of $a(x)$ and $b(x)$ injected on the diagonal.

Applying the energy method by multiplying (4) by $v_t^T H$ and adding the transpose leads to

$$\begin{aligned} \frac{d}{dt} (\|v\|_{H_a}^2 + \|D_1 v\|_{H_b}^2) &= -(v_t)_0^T (2 - 2\tau) (B D_1 v)_0 + (v_t)_N^T (2 - 2\tau) (B D_1 v)_N \\ &\quad + 2\tau (v_t)_0^T (g - \alpha v_t)_0 + 2\tau (v_t)_N^T (g - \alpha v_t)_N. \end{aligned}$$

Setting $\tau = 1$ leads to

$$\frac{d}{dt} (\|v\|_{H_a}^2 + \|D_1 v\|_{H_b}^2) = -2 (v_t)_0^T (\alpha v_t - g)_0 - 2 (v_t)_N^T (\alpha v_t - g)_N. \quad (5)$$

Equation (5) exactly mimics (3), except for the highest frequency mode (see [18]). The problems with the numerical scheme given by (4) are twofold: 1) It does not damp the highest frequency mode (see for example first row in Figure 4), which can be proven with Fourier analysis [18]. 2) For a given order of accuracy, the internal numerical scheme is wider than necessary, leading to lower than optimal numerical accuracy. A remedy would be to employ a narrow-stencil SBP operator for $\partial/\partial x (b \partial/\partial x)$, where $b(x) > 0$.

In [16] we introduced the following definition:

Definition 2.3 Let $D_2^{(b)} = H^{-1}(-M^{(b)} + \bar{B}S)$ approximate $\partial/\partial x (b \partial/\partial x)$, where $b(x) > 0$, using a p th-order accurate narrow-stencil. $D_2^{(b)}$ is said to be a p th-order accurate narrow-diagonal second-derivative SBP operator, if H is diagonal and positive definite, $M^{(b)}$ is symmetric and positive semi-definite, S approximates the first-derivative operator at the boundaries and $\bar{B} = \text{diag}(-b_0, 0, \dots, 0, b_N)$.

Definition 2.3 present a somewhat more vague approximation of $\partial/\partial x (b \partial/\partial x)$, since the matrix $M^{(b)}$ is only known to be positive semidefinite (see [17]). In [17] we introduced a property referred to as *complete* for constant coefficient second-derivative SBP operators. The following property is a direct extension to the variable coefficient case:

Definition 2.4 Let $D_2^{(b)}$ be a p th-order accurate narrow-diagonal second-derivative SBP operators. If $M^{(b)} = h D^T \tilde{B} D$, where D is a consistent approximation of $\partial/\partial x$ and \tilde{B} is a diagonal representation of $b(x)$, $D_2^{(b)}$ is called *complete*.

By employing a narrow-diagonal SBP operator $D_2^{(b)}$ in (2), we obtain the semi-discrete approximation

$$\begin{aligned} Av_{tt} = D_2^{(b)} v & -H^{-1}\tau e_0 \{(\alpha v_t - B S v)_0 - g\} \\ & -H^{-1}\tau e_N \{(\alpha v_t + B S v)_N - g\} . \end{aligned} \quad (6)$$

Applying the energy method by multiplying (6) by $v_t^T H$, adding the transpose and setting $\tau = 1$ leads to

$$\frac{d}{dt} (\|v\|_{H_a}^2 + v_t^T M^{(b)} v_t) = -2 (v_t^T (\alpha v_t - g))_0 - 2 (v_t^T (\alpha v_t - g))_N . \quad (7)$$

Equation (7) is a semi-discrete analogue to (3), also for the highest frequency mode. (If we employ a complete SBP operator (7) exactly mimics (12).)

The advantages of employing narrow-diagonal second-derivative SBP operators are that they damp the highest frequency mode, and yield a more accurate representation of $\partial/\partial x (b \partial/\partial x)$. However, such operator have not yet been presented in literature, except for second-order accuracy [16] where it was shown to be also complete since $M^{(b)} = D^T \tilde{B} D$, where

$$D = \frac{1}{h} \begin{bmatrix} -1 & 1 & & & & \\ & -1 & 1 & & & \\ & & & \ddots & & \\ & & & & -1 & 1 \\ & & & & -1 & 1 \end{bmatrix}, \quad \tilde{B} = \frac{h}{2} \begin{bmatrix} b_0 + b_1 & & & & & \\ & b_1 + b_2 & & & & \\ & & \ddots & & & \\ & & & & b_{N-1} + b_N & \\ & & & & & 0 \end{bmatrix} .$$

In [11] the variable coefficient problem (for the second, fourth and sixth-order case) was analyzed without inclusion of boundaries (i.e., not SBP) and mixed second-derivative terms.

Remark To obtain energy estimates for schemes utilizing both D_1 and $D_2^{(b)}$ requires that both are based on the same norm H .

Remark The boundary closure for a p th-order accurate narrow-diagonal SBP operator is of order $p/2$ (see [17]). The convergence rate for narrow-stencil approximations of second-order hyperbolic problems drops to $(p/2 + 2)$ th-order. (See [8, 27] for more information on the accuracy of finite difference approximations.)

It was shown in [19] that the present Definitions 2.3 and 2.4 of a narrow-diagonal second-derivative SBP operators alone does not guarantee stability for problems with a combination of mixed $(\partial^2/\partial x \partial y)$ and non-mixed $(\partial^2/\partial x^2, \partial^2/\partial y^2)$ second-derivatives, such as the compressible Navier-Stokes equations [19] and the elastic wave equation [1]. In [19] we introduced an important relationship between the existing narrow-diagonal first- and second-derivative (first derived in [17]) SBP operators, referred to as *compatibility*. The main result of that study was to show that compatibility is required to prove stability for problems with a combination of mixed and non-mixed second-derivatives. That study focused on the constant coefficient problems since high-order accurate compatible second-derivative SBP operators with variable coefficients at the time did not exist.

2.2 Two-Dimensional Domains

To simplify the 2-D analysis we introduce some notation, beginning with the Kronecker product:

$$C \otimes D = \begin{bmatrix} c_{0,0} D & \cdots & c_{0,q-1} D \\ \vdots & & \vdots \\ c_{p-1,0} D & \cdots & c_{p-1,q-1} D \end{bmatrix},$$

where C is a $p \times q$ matrix and D is an $m \times n$ matrix. Two useful rules for the Kronecker product are $(A \otimes B)(C \otimes D) = (AC) \otimes (BD)$ and $(A \otimes B)^T = A^T \otimes B^T$.

The following definition will be used in subsequent sections:

Definition 2.5 Let $\bar{x} = (x, y)$ denote grid coordinates in two dimensions. We define the 2-D bounding box $0 \leq x \leq 1$, $0 \leq y \leq 1$ by $\bar{x} \in \Omega$, and the line $x = 1$, $0 \leq y \leq 1$ by $\bar{x} \in \Omega_{East}$.

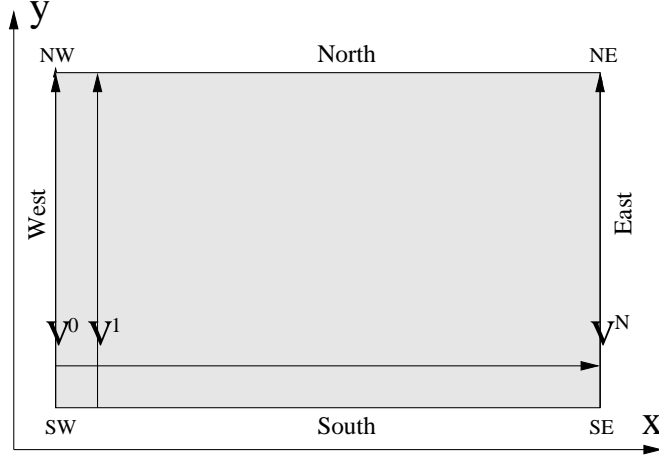


Figure 1: Domain 2-D

The domain Ω is discretized with an $(N + 1) \times (M + 1)$ -point equidistant grid defined as

$$\begin{aligned} x_i &= 0 + ih_x, \quad i = 0, 1, \dots, N, \quad h_x = \frac{1}{N}, \\ y_j &= 0 + jh_y, \quad j = 0, 1, \dots, M, \quad h_y = \frac{1}{M}. \end{aligned}$$

To simplify notation (without any restriction) we assume the same dimension (N) in both the x - and y -direction. The numerical approximation at grid point $(x_i, y_j) \equiv \bar{x}_{i,j}$ is a $1 \times k$ -vector denoted $v_{i,j}$. The tensor product derivations are more transparent if we redefine the component vector $v_{i,j}$ as a “vector of vectors.” Specifically, define a discrete solution vector $v^T = [v^0, v^1, \dots, v^N]$, where $v^p = [v_{p,0}, v_{p,1}, \dots, v_{p,N}]$ is the solution vector at x_p along the y -direction, see Figure 1. To distinguish whether a 2-D difference operator P is operating in the x - or the y -direction, we use the notations P_x and P_y , respectively. The following 2-D operators are frequently used:

$$\begin{aligned} D_x &= I_k \otimes D_1 \otimes I_N, & D_y &= I_k \otimes I_N \otimes D_1 \\ D_{2x}^{(b)} &= I_k \otimes D_2^{(b)} \otimes I_N, & D_{2y}^{(b)} &= I_k \otimes I_N \otimes D_2^{(b)} \\ R_x^{(b)} &= I_k \otimes R^{(b)} \otimes I_N, & R_y^{(b)} &= I_k \otimes I_N \otimes R^{(b)} \\ S_x &= I_k \otimes S \otimes I_N, & S_y &= I_k \otimes I_N \otimes S \\ B_x &= I_k \otimes B \otimes I_N, & B_y &= I_k \otimes I_N \otimes B \\ \bar{B}_x &= I_k \otimes \bar{B} \otimes I_N, & \bar{B}_y &= I_k \otimes I_N \otimes \bar{B} \\ H_x &= I_k \otimes H \otimes I_N, & H_y &= I_k \otimes I_N \otimes H \\ e_{West} &= I_k \otimes e_0 \otimes I_N, & e_{South} &= I_k \otimes I_N \otimes e_0 \\ e_{East} &= I_k \otimes e_N \otimes I_N, & e_{North} &= I_k \otimes I_N \otimes e_N \\ \tilde{H} &= H_x H_y & \hat{H} &= \text{diag}(\tilde{H}, \tilde{H}) \end{aligned}, \quad (8)$$

where $D_1, D_2^{(B)}, S, R, B, \bar{B}$ and H are the 1-D operators introduced in this section and the next. Note that $D_{2x}^{(b)} = H_x^{-1}(-D_x^T B_x H_x D_x - R_x^{(b)} + \bar{B}_x S_x)$, $D_{2y}^{(b)} = H_y^{-1}(-D_y^T B_y H_y D_y - R_y^{(b)} + \bar{B}_y S_y)$. I_N and I_k are identity matrices of appropriate sizes, and e_0 and e_N are 1-D “boundary” vectors defined by (1).

3 Compatible second-derivative SBP operators

The main goal of the present study is to derive and construct high-order accurate compatible narrow-diagonal SBP operators for second-derivatives with variable coefficients. The following definition is central in this paper:

Definition 3.1 *Let D_1 and $D_2^{(b)}$ be p th-order accurate narrow-diagonal first- and second-derivative SBP operators. If $M^{(b)} = D_1^T H B D_1 + R^{(b)}$, and the remainder $R^{(b)}$ is positive semi-definite, D_1 and $D_2^{(b)}$ are called compatible.*

The study of the constant coefficient problem in [19] gave an idea to the following ansatz for the remainders $R^{(b)}$ in the corresponding variable coefficient case, for the second, fourth, sixth and eighth-order cases (starting with the second-order case and ending with the eighth-order case below):

$$\begin{aligned}
R^{(b)} &= \frac{h^3}{4} (D_2^{(2)})^T C_2^{(2)} B D_2^{(2)} \\
R^{(b)} &= \frac{h^5}{18} (D_3^{(4)})^T C_3^{(4)} B D_3^{(4)} + \frac{h^7}{144} (D_4^{(4)})^T C_4^{(4)} B D_4^{(4)} \\
R^{(b)} &= \frac{h^7}{80} (D_4^{(6)})^T C_4^{(6)} B D_4^{(6)} + \frac{h^9}{600} (D_5^{(6)})^T C_5^{(6)} B D_5^{(6)} + \frac{h^{11}}{3600} (D_6^{(6)})^T C_6^{(6)} B D_6^{(6)} \\
R^{(b)} &= \frac{h^9}{350} (D_5^{(8)})^T C_5^{(8)} B D_5^{(8)} + \frac{h^{11}}{2520} (D_6^{(8)})^T C_6^{(8)} B D_6^{(8)} + \frac{h^{13}}{14700} (D_7^{(8)})^T C_7^{(8)} B D_7^{(8)} \\
&\quad + \frac{h^{15}}{78400} (D_8^{(8)})^T C_8^{(8)} B D_8^{(8)}.
\end{aligned} \tag{9}$$

The internal schemes in $D_i^{(p)}$ ($p = 2, 4, 6, 8$, denoting different order of accuracy) are narrow-stencil approximations of $\frac{d^i}{dx^i}$ and $C_i^{(p)}$ are diagonal matrices with non-negative entries, $i = 2, \dots, 8$. Note that $D_i^{(p)}$ for different orders of accuracy p differ only at the boundaries for a given derivative order (denoted by i). Note that this ansatz guarantee that $R^{(b)}$ is symmetric and positive semidefinite by construction, up to eighth-order.

The interior scheme is given, since we require minimal width and p th-order accuracy. Left to find are the boundary modifications in $D_i^{(p)}$ and $C_i^{(p)}$ such that the following constraints are met:

1. $D_2^{(b)}$, when $b(x) = 1$, is identical to the compatible constant coefficient second-derivative SBP operators first derived in [17].

2. $C_i^{(p)}$ has non-negative entries.
3. $D_i^{(p)}$ is a consistent approximation of $\frac{d^i}{dx^i}$ at the boundaries.
4. $D_2^{(b)}$ is of order $p/2$ at the boundaries.

Altogether, the above ansatz and constraints lead to a large non-linear system of equations, especially for the sixth and eighth-order cases. Typically you need to reduce as much as possible the number of unknowns (in a way that still allows a solution). The first step is to restrict the unknowns in $D_i^{(p)}$ and $C_i^{(p)}$, such that the first three constraints above are met. The most difficult part is to find a valid solution such that the entries in $C_i^{(p)}$ are non-negative. A fruitful approach (found after some testing) is to set as many entries as possible to zero in $C_i^{(p)}$ close to the boundaries and just allow unknowns in a few rows in $D_i^{(p)}$ (typically corresponding to the rows with the unknown entries in $C_i^{(p)}$). Start with as few unknowns as possible (you need at least as many as there are equations). If no solution is found, more unknowns are introduced. If any unknowns are left after fulfilling the first three constraints, they are used to guarantee that the last constraint is met.

After some extensive testing, compatible SBP operators are derived (see Definition 3.1) fulfilling the four constraints above for the second-, fourth- and sixth-order cases, by using the symbolic mathematics software Maple, see Appendix I. Strictly speaking the first constraint is not necessary, but it do guarantee that the operators are well behaved, meaning that the spectral radius is small (see, for example, [26]) and that the boundary accuracy is high. In the eighth-order case a solution fulfilling the first constraint could not be found, which is why we omit presenting the result for the eighth-order case. It is an open question if a solution exists for the eighth-order case fulfilling the first constraint.

4 Analysis

In [19] we introduced a property referred to as *compatible* SBP operators, a necessary condition proving stability using the energy method for narrow-stencil finite difference approximations of PDEs involving mixed and non-mixed second-derivative terms. In that study, only constant coefficient problems were analyzed in detail, since compatible SBP operators for variable coefficients did not exist.

Our main focus in the present study is on deriving narrow-stencil high-order accurate compatible second-derivative SBP operators with variable

coefficients. These operators are necessary in order to derive strictly stable narrow-stencil approximations for problems with a combination of mixed $\partial/\partial x (b_{12}(x, y) \partial/\partial y)$, $\partial/\partial y (b_{21}(x, y) \partial/\partial x)$ and pure $\partial/\partial x (b_{11}(x, y) \partial/\partial x)$, $\partial/\partial y (b_{22}(x, y) \partial/\partial y)$ second-derivatives with variable coefficients, such as the compressible Navier-Stokes equations and various second-order hyperbolic systems on curvilinear grids.

Consider the 2-D hyperbolic system (with k unknowns):

$$Au_{tt} = (C_{11}u_x + C_{12}u_y)_x + (C_{21}u_x + C_{22}u_y)_y, \quad \bar{x} \in \Omega. \quad (10)$$

We Introduce

$$C = \begin{bmatrix} C_{11} & C_{12} \\ C_{21} & C_{22} \end{bmatrix}, \quad \hat{u} = \begin{bmatrix} u_x \\ u_y \end{bmatrix},$$

and require the $2k \times 2k$ matrix C to be symmetric and positive semidefinite. The discrete counterpart to \hat{u} is given by

$$\hat{v} = \begin{bmatrix} D_x v \\ D_y v \end{bmatrix}.$$

We consider the following boundary conditions at the 4 boundaries (East, West, North, South):

$$\begin{aligned} \Phi_{East}u_t + C_{11}u_x + C_{12}u_y &= g, \quad \bar{x} \in \Omega_{East} \\ \Phi_{West}u_t - C_{11}u_x - C_{12}u_y &= g, \quad \bar{x} \in \Omega_{West} \\ \Phi_{North}u_t + C_{21}u_x + C_{22}u_y &= g, \quad \bar{x} \in \Omega_{North} \\ \Phi_{South}u_t - C_{21}u_x - C_{22}u_y &= g, \quad \bar{x} \in \Omega_{South}. \end{aligned} \quad (11)$$

Remark Other type of well-posed boundary conditions, like Dirichlet can also be used. However, the main focus in this paper is on the derivation of compatible second-derivative SBP operators.

Multiplying Eq. 10 by u_t , and integrating by parts with the use of (11) lead to

$$E_t = BT_{East} + BT_{West} + BT_{North} + BT_{South}, \quad (12)$$

where

$$E = \int \int_{\Omega} u_t^T A u_t + \bar{u}^T C \bar{u} \, dx \, dy, \quad (13)$$

and

$$\begin{aligned} BT_{East} &= -2 \int_{\partial\Omega_{East}} u_t^T (\Phi_{East}u_t - g) \, dy, \\ BT_{West} &= -2 \int_{\partial\Omega_{West}} u_t^T (\Phi_{West}u_t - g) \, dy, \\ BT_{North} &= -2 \int_{\partial\Omega_{North}} u_t^T (\Phi_{North}u_t - g) \, dx, \\ BT_{South} &= -2 \int_{\partial\Omega_{South}} u_t^T (\Phi_{South}u_t - g) \, dx. \end{aligned} \quad (14)$$

An energy estimate exists if $\Phi_{East, West, North, South}$ are positive semidefinite.

A corresponding semi-discrete approximation of (10) with the boundary conditions (11) can be written

$$A v_{tt} = D_x (C_{11} D_x v + C_{12} D_y v) + D_y (C_{21} D_x v + C_{22} D_y v) + SAT_{E, W, N, S}, \quad (15)$$

where $SAT_{E, W, N, S}$ imposes the boundary conditions (11) using the penalty technique

$$\begin{aligned} SAT_E &= -H_x^{-1} e_{East} ((\Phi_{East} v_t + C_{11} D_x v + C_{12} D_y v)_E - g), \\ SAT_W &= -H_x^{-1} e_{West} ((\Phi_{West} v_t - C_{11} D_x v - C_{12} D_y v)_W - g), \\ SAT_N &= -H_y^{-1} e_{North} ((\Phi_{North} v_t + C_{21} D_x v + C_{22} D_y v)_N - g), \\ SAT_S &= -H_y^{-1} e_{South} ((\Phi_{South} v_t + C_{21} D_x v + C_{22} D_y v)_S - g). \end{aligned}$$

In the following, the subscripts E, W, N, S indicates that the quantities reside on the East, West, North and South boundaries (see Figure 1).

Apply the energy method by multiplying (15) by $v_t^T \tilde{H}$, and adding the transpose, leading to (12), where now

$$E = v_t^T A \tilde{H} v_t + \hat{v}^T C \hat{H} \hat{v}, \quad (16)$$

and

$$\begin{aligned} BT_{East} &= -2 (v_t^T H_y (\Phi_{East} v_t - g))_E, \\ BT_{West} &= -2 (v_t^T H_y (\Phi_{West} v_t - g))_W, \\ BT_{North} &= -2 (v_t^T H_x (\Phi_{North} v_t - g))_N, \\ BT_{South} &= -2 (v_t^T H_x (\Phi_{South} v_t - g))_S. \end{aligned} \quad (17)$$

Hence, the semi-discrete energy estimate exactly mimic the continuous energy estimate, except for the highest frequency mode. This can potentially alter the scheme unstable. The reason for this is that the first derivative SBP operator used to build the energy term $\hat{v}^T C \hat{H} \hat{v}$ in (16) does not damp spurious oscillations (i.e., the highest frequency mode).

Remark The compatible narrow-stencil second-derivative SBP operators are constructed to mimic the continuous energy estimate for problems such as (10), and introduce a mechanism for damping the highest frequency mode.

A semidiscretization of (10) using compatible narrow-diagonal SBP operators and the SAT method can be written as

$$A v_{tt} = D_{2x}^{(C_{11})} v + D_x C_{12} D_y v + D_y C_{21} D_x v + D_{2y}^{(C_{22})} v + \tilde{S}AT_{E, W, N, S}, \quad (18)$$

where $\tilde{S}AT_{E, W, N, S}$ are given by

$$\begin{aligned} \tilde{S}AT_E &= -H_x^{-1} e_{East} ((\Phi_{East} v_t + C_{11} S_x v + C_{12} D_y v)_E - g), \\ \tilde{S}AT_W &= -H_x^{-1} e_{West} ((\Phi_{West} v_t - C_{11} S_x v - C_{12} D_y v)_W - g), \\ \tilde{S}AT_N &= -H_y^{-1} e_{North} ((\Phi_{North} v_t + C_{21} D_x v + C_{22} S_y v)_N - g), \\ \tilde{S}AT_S &= -H_y^{-1} e_{South} ((\Phi_{South} v_t + C_{21} D_x v + C_{22} S_y v)_S - g). \end{aligned}$$

(The differences between (15) and (18) is that we have replaced $D_x C_{11} D_x$, and $D_y C_{22} D_y$ with $D_{2x}^{(C_{11})}$ and $D_{2y}^{(C_{22})}$ respectively, and that we have replaced D_x and D_y with S_x and S_y at the appropriate places in the penalty terms.)

One of the main results of this paper is stated in the following theorem:

Theorem 4.1 *The scheme (18) is strictly stable if D_1 , $D_2^{(C_{22})}$ and $D_2^{(C_{11})}$ are compatible narrow-diagonal first- and second-derivative SBP operators and $\Phi_{East, West, North, South}$ are positive semidefinite.*

Proof Multiplying (18) by $v_t^T \tilde{H}$ from the left and adding the transpose lead to

$$E_t = BT_{East} + BT_{West} + BT_{North} + BT_{South} ,$$

where

$$E = v_t^T A \tilde{H} v_t + \hat{v}^T C \hat{H} \hat{v} + v^T H_y R_x^{(C_{11})} v + v^T H_x R_y^{(C_{22})} v ,$$

and

$$\begin{aligned} BT_{East} &= -2 \left(v_t^T H_y (\Phi_{East} v_t - g) \right)_E , \\ BT_{West} &= -2 \left(v_t^T H_y (\Phi_{West} v_t - g) \right)_W , \\ BT_{North} &= -2 \left(v_t^T H_x (\Phi_{North} v_t - g) \right)_N , \\ BT_{South} &= -2 \left(v_t^T H_x (\Phi_{South} v_t - g) \right)_S . \end{aligned}$$

The semi-discrete energy estimate exactly mimics the continuous energy estimate iff $R_x^{(C_{11})}$ and $R_y^{(C_{22})}$ are positive semi-definite. Since D_1 , $D_2^{(C_{22})}$ and $D_2^{(C_{11})}$ are compatible stability follows if $\Phi_{East, West, North, South}$ are positive semidefinite. \square

Remark The additional (small) energy terms $v^T H_y R_x^{(C_{11})} v$ and $v^T H_x R_y^{(C_{22})} v$ in Theorem 4.1 introduce a mechanism for efficient damping of spurious oscillations, without destroying accuracy and the energy estimate.

Remark Theorem 4.1 shows why it is necessary to employ compatible narrow-diagonal SBP operators (see Definition 3.1) to exactly mimic the continuous energy estimate for multi-D problem consisting of mixed and pure second-derivative terms, and hence proving strict stability.

5 Efficiency study

The main focus in the present study is to construct compatible narrow-diagonal SBP operators for variable coefficient second derivatives, necessary when proving stability for general multi-D problems involving variable coefficient mixed and non-mixed second-derivatives. The necessary stability constraints (see Definition 3.1) can only be seen in a multi-D setting, proven

in Theorem 4.1. The main difference between the narrow-stencil and the corresponding wide-stencil approximation (i.e., when employing only the first derivative SBP operator) lies in the treatment of the pure second-derivative terms (such as $(C_{11}u_x)_x$ and $(C_{22}u_y)_y$ in (10)). To motivate numerically the use for narrow-diagonal SBP operators we will compare the accuracy- and stability-properties of the corresponding wide-stencil approximation in a 1-D setting. In a coming study we will do a similar study in multi-D.

The convergence rate is calculated as

$$q = \log_{10} \left(\frac{\|u - v^{(N_1)}\|_h}{\|u - v^{(N_2)}\|_h} \right) / \log_{10} \left(\frac{N_1}{N_2} \right)^{1/d}, \quad (19)$$

where d is the dimension ($d = 1$ in the 1-D case), u is the analytic solution, and $v^{(N_1)}$ the corresponding numerical solution with N_1 unknowns. $\|u - v^{(N_1)}\|_h$ is the discrete l_2 norm of the error.

We study the 1-D wave equation (2), where the coefficients $a_1(x)$, $a_2(x) > 0$ are discontinuous at $x = 0$, leading to the following problem

$$\begin{aligned} a^{(1)}u_{tt}^{(1)} &= (b^{(1)}u_x^{(1)})_x, & -1 \leq x \leq 0 \\ a^{(2)}u_{tt}^{(2)} &= (b^{(2)}u_x^{(2)})_x, & 0 \leq x \leq 1 \end{aligned}, \quad (20)$$

where $a^{(1)} \neq a^{(2)}$, $b^{(1)} \neq b^{(2)}$. Here $u^{(1,2)}$ denote the solutions corresponding to the left and right domains respectively. We introduce the following coordinate transformations,

$$\begin{aligned} x = x(\xi) &= \xi \left(\frac{e^{-(\xi+\frac{4}{5})^2}}{e^{-(-1+\frac{4}{5})^2}} \right)^l, & \xi = [-1, 0], \\ x = x(\xi) &= \xi \left(\frac{e^{-(\xi-\frac{4}{5})^2}}{e^{-(1-\frac{4}{5})^2}} \right)^l, & \xi = [0, 1], \end{aligned} \quad (21)$$

in the left and right domains, respectively. Here l is a non-negative integer, where the case $l = 0$ corresponds to the cartesian case. (A larger value on l leads to a denser clustering of grid-points close to the interface and the outer boundaries, see Figure 2.) The problem (20) transforms to

$$\begin{aligned} \tilde{a}^{(1)}u_{tt}^{(1)} &= (c^{(1)}u_\xi^{(1)})_\xi, & -1 \leq \xi \leq 0 \\ \tilde{a}^{(2)}u_{tt}^{(2)} &= (c^{(2)}u_\xi^{(2)})_\xi, & 0 \leq \xi \leq 1 \end{aligned}, \quad (22)$$

in curvilinear coordinates, where $\tilde{a}^{(1,2)} = a^{(1,2)}x_\xi^{(1,2)}$ and $c^{(1,2)} = b^{(1,2)}/x_\xi^{(1,2)}$. Continuity at the interface ($\xi = 0$) means that the following interface (jump) conditions:

$$u^{(1)} = u^{(2)}, \quad c^{(1)}u_\xi^{(1)} = c^{(2)}u_\xi^{(2)}, \quad (23)$$

have to be imposed. The SAT method of handling discontinuous media is used. To make the paper self contained we write out in detail the SBP-SAT treatment of the 1-D model problem. (A detailed analysis of this particular problem is described in [16].) The semi-discrete approximation of (23) can be written

$$I_1 \equiv v_N^{(1)} - v_0^{(2)} = 0 \quad I_2 \equiv (\bar{C}^{(1)} S v^{(1)})_N + (\bar{C}^{(2)} S v^{(2)})_0 = 0 \quad . \quad (24)$$

Here $v^{(1,2)}$ are the solution vectors corresponding to the left and right domains respectively. The left and right domains are discretized using $(N + 1)$ grid points.

A semi-discretization of the Neumann boundary conditions (that are applied at the outer boundaries) are given by

$$L_1^T v^{(1)} = (\bar{C}^{(1)} S v^{(1)})_N = g \quad , \quad L_2^T v^{(2)} = (\bar{C}^{(2)} S v^{(2)})_0 = g \quad . \quad (25)$$

A semi-discretization of Eq. 22 using narrow-diagonal SBP operators and the SAT method to impose the semi-discrete interface conditions (24) and boundary conditions (25), can be written:

$$\begin{aligned} \tilde{A}_1 v_{tt}^{(1)} &= D_2^{(c^{(1)})} v^{(1)} & \tilde{A}_2 v_{tt}^{(2)} &= D_2^{(c^{(2)})} v^{(2)} \\ &+ \tau H^{-1} e_N(I_1) & &- \tau H^{-1} e_0(I_1) \\ &+ \beta (\bar{C}^{(1)} S)^T e_N H^{-1}(I_1) & &- \beta (\bar{C}^{(2)} S)^T e_0 H^{-1}(I_1) \\ &+ \gamma H^{-1} e_N(I_2) & &- \gamma H^{-1} e_0(I_2) \\ &- H^{-1} e_0(L_1^T v^{(1)} - g_{-1}) & &+ H^{-1} e_N(L_2^T v^{(2)} - g_1) \end{aligned} \quad (26)$$

The following Lemma was first stated in [16]:

Lemma 5.1 *The scheme (26) is strictly stable if $D_2^{c^{(1,2)}}$ are narrow-diagonal SBP operators, $\gamma = -\frac{1}{2}$, $\beta = \frac{1}{2}$ and $\tau \leq -\frac{c^{(1)}+c^{(2)}}{4h\alpha}$ hold.*

The proof can be found in [16], where the value of $\alpha = 0.1878715026$ (in the above lemma) is shown for the sixth order case.

5.1 Accuracy property

In the first test the accuracy properties of the sixth-order accurate wide- and narrow-stencil approximations are compared, for an analytic standing wave solution given by

$$\begin{aligned} u^{(1)} &= \cos(\sqrt{\pi b^{(1)} a^{(1)}} t) \cos(\pi a^{(1)} \xi), \quad \xi = [-1, 0], \\ u^{(2)} &= \cos(\sqrt{\pi b^{(2)} a^{(2)}} t) \cos(\pi a^{(2)} \xi), \quad \xi = [0, 1] \quad . \end{aligned} \quad (27)$$

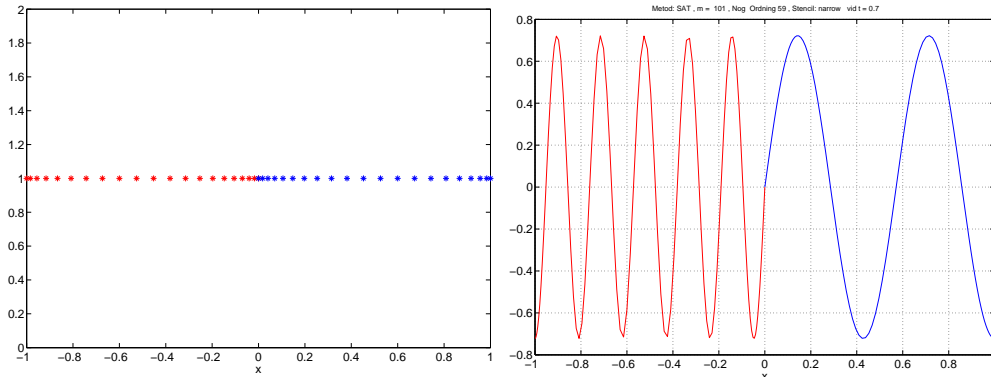


Figure 2: The stretched grid (corresponding to $l = 2$ in Eq. 21) in the left subfigure, and the numerical solution to the standing wave problem (given by Eq. 27) at $t=0.7$ using the sixth-order accurate narrow-stencil SBP-SAT method (right) .

N	$\log l_2^{(l=0)}$	$q^{(l=0)}$	$\log l_2^{(l=1)}$	$q^{(l=1)}$	$\log l_2^{(l=2)}$	$q^{(l=2)}$
51	-2.29	0.00	-2.94	0.00	-2.64	0.00
101	-4.20	6.43	-4.74	6.07	-4.40	5.92
201	-5.91	5.72	-6.54	6.01	-6.19	5.98
401	-7.58	5.59	-8.30	5.86	-7.92	5.79
801	-9.22	5.46	-10.07	5.90	-9.68	5.84

Table 1: $\log(l_2 - errors)$ and convergence rates for different grid-stretching l (see Eq. 21) in the first test. Sixth-order accurate narrow-stencil.

The analytic solution is constructed such that $u_\xi \neq 0$ at the interface ($\xi = 0$) by choosing $a^{(1)} = 10 + 1/2$, $a^{(2)} = 3 + 1/2$, $b^{(1)} = a^{(2)}$ and $b^{(2)} = a^{(1)}$. At the outer boundaries we impose homogenous Neumann boundary conditions. The numerical approximation is run to $t = 0.7$, using a time step $dt = 10^{-4}$. We use a compact fourth-order accurate time discretization (see [16] for details). The convergence study for the sixth-order accurate narrow- and wide-stencil approximations are presented in Tables 1 and 2 respectively.

The conclusion of this first test is that the narrow-stencil approximation is much more efficient than the corresponding wide-stencil approximation. We should mention that the time-step restrictions of the wide- and narrow-stencil approximations are approximately the same.

N	$\log l_2^{(l=0)}$	$q^{(l=0)}$	$\log l_2^{(l=1)}$	$q^{(l=1)}$	$\log l_2^{(l=2)}$	$q^{(l=2)}$
51	-1.25	0.00	-1.75	0.00	-1.69	0.00
101	-2.56	4.41	-3.27	5.15	-3.41	5.80
201	-3.86	4.34	-4.87	5.34	-5.10	5.66
401	-5.30	4.83	-6.30	4.76	-6.59	4.96
801	-6.72	4.71	-7.66	4.52	-7.89	4.31

Table 2: $\log(l_2 - errors)$ and convergence rates for different grid-stretching l (see Eq. 21) in the first test. Sixth-order accurate wide-stencil.

N	$\log l_2^{(narrow)}$	$q^{(narrow)}$	$\log l_2^{(wide)}$	$q^{(wide)}$
101	-1.39		-1.07	
201	-2.31	3.12	-1.72	2.17
401	-4.23	6.43	-3.30	5.29
801	-6.14	6.37	-4.68	4.62

Table 3: $\log(l_2 - errors)$ and convergence rates for the sixth-order SAT method in the second test, comparing the narrow- and wide-stencil approximations.

5.2 Stability property

In the second test we focus on the stability properties of the narrow- and wide-stencil approximations. In particular the SAT method of handling the discontinuous media (see [16] for details) interface is compared to the method of differentiating across the discontinuity here referred to as the "Ignoring" method. Again the model-problem is given by Eq. 20, where $a^{(1)} = 1$, $a^{(2)} = 2$, $b^{(1)} = 2$ and $b^{(2)} = 8$. We now run a Gaussian initial profile to $t = 10$ (see Figure 3). The reference solution is recorded using 1601 grid-points in each domain. In Table 3 we compare the narrow- and wide-stencil approximations, treating the media jump with the SAT method, using sixth-order accurate SBP operators and a compact fourth-order time-discretization.

In Table 4 we compare the narrow- and wide-stencil approximations when ignoring the media jump, which leads to first-order accurate approximations (see [10] for a detailed convergence study on this problem). In Figure 4 we present the numerical solutions at $t = 10$ using 101 and 201 grid points in each domain, comparing both the wide- and narrow-stencil approximations with and without the SAT treatment. The highest frequency mode is clearly visible in the wide-stencil approximations of the ignoring method (presented in the first row in Figure 4). In Table 5 we compare the narrow- and wide-stencil approximations when ignoring the media jump for the corresponding

N	$\log l_2^{(narrow)}$	$q^{(narrow)}$	$\log l_2^{(wide)}$	$q^{(wide)}$
101	-0.96		-0.94	
201	-1.15	0.64	-1.03	0.28
401	-1.47	1.05	-1.33	1.00
801	-1.78	1.06	-1.66	1.12

Table 4: $\log(l_2 - errors)$ and convergence rates for the sixth-order Ignoring method in the second test, comparing the narrow- and wide-stencil approximation.

N	$\log l_2^{(SAT)}$	$q^{(SAT)}$	$\log l_2^{(Ignoring)}$	$q^{(Ignoring)}$
101	-0.76		-0.94	
201	-0.88	0.40	-0.99	0.18
401	-1.08	0.69	-1.16	0.58
801	-1.64	1.84	-1.67	1.67
1601	-2.23	1.99	-2.15	1.60

Table 5: $\log(l_2 - errors)$ and convergence rates for the second-order SAT and Ignoring method in the second test, using narrow-stencil approximations.

second-order case, which is the most widely used finite difference approximation in practical applications.

The conclusion of this last study can be summarized in the following: 1) It is very important to use the SAT method of handling the media jump, 2) The narrow-stencil approximation is much more efficient than the corresponding wide-stencil approximation, and 3) If ignoring the media jump, a second-order finite difference scheme can be more efficient than a corresponding higher-order scheme.

6 Conclusions

Our approach has been to construct narrow-stencil SBP operators for variable coefficient second-derivatives, with a property referred to as compatibility. Together with the SAT technique to impose boundary and interface conditions, strict stability can be shown using the energy method, for general second-order hyperbolic (and parabolic) problems. The main objective was to construct SBP operators that combined the following desirable properties:

- stability by construction in combination with the existing first derivative SBP operators,
- capable of maintaining the overall convergence rate,

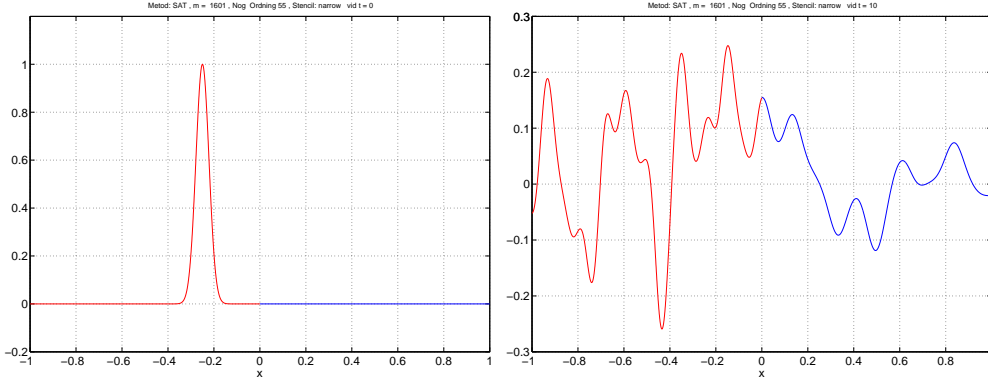


Figure 3: Solution at $t = 10$ (right), using the sixth-order accurate narrow-stencil SBP-SAT method, initiated with a Gaussian profile (left). $N = 1601$ in each subdomain.

- capable of maintaining simplicity of the numerical scheme.

To achieve the three properties above, we have constructed SBP operators with the following requirements: (1) We mimic the continuous energy estimate for general second-order 2-D problems (the extension to 3-D is straightforward) by requiring compatibility with the first derivative SBP operators. (2) They have the same order of accuracy as the corresponding wide-stencil approximation. (3) They are of minimal width in the interior.

Numerical computations in 1-D corroborate the stability- and accuracy-properties and also show that narrow-stencil approximations are more accurate and robust than the corresponding wide stencil approximations.

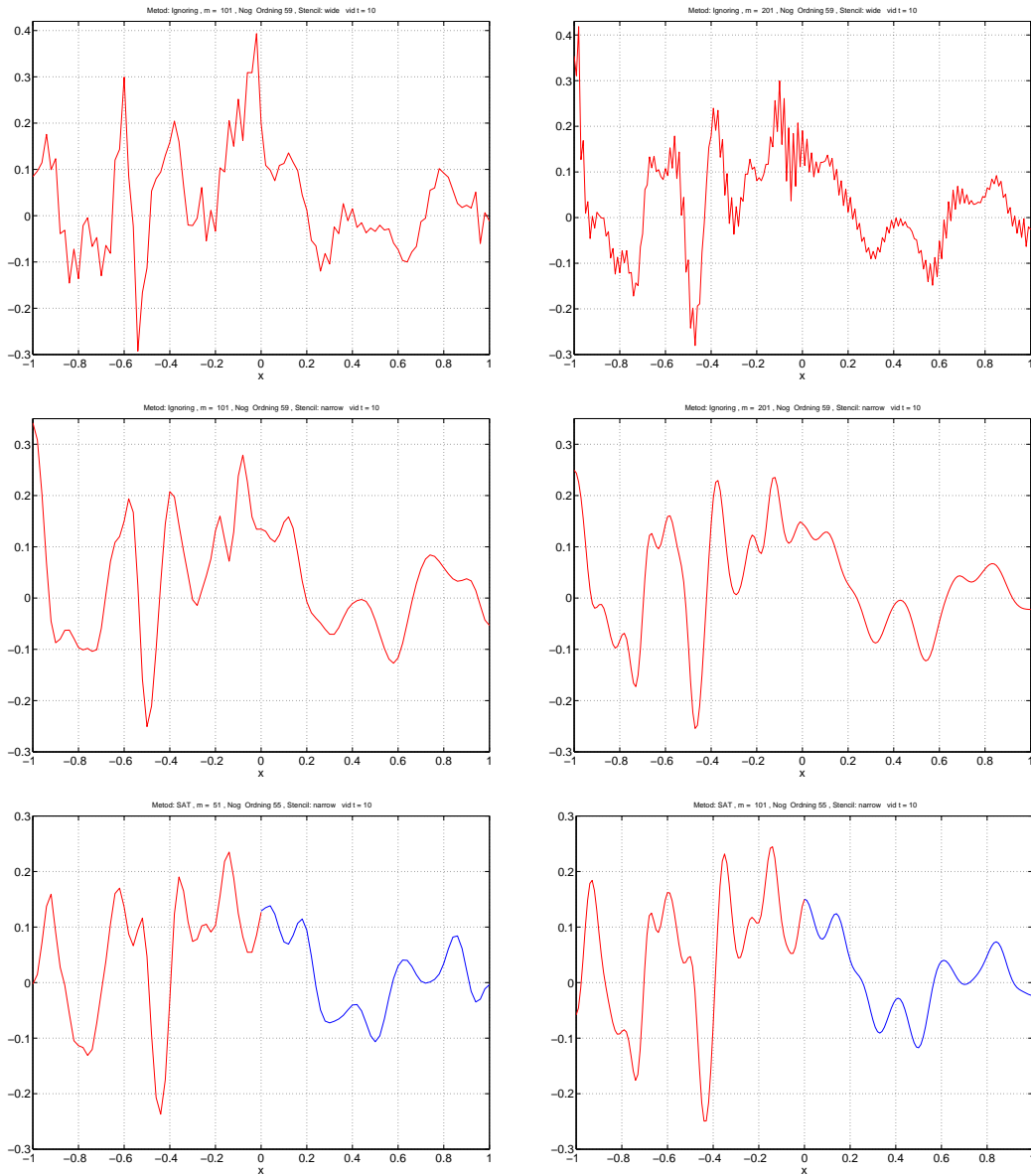


Figure 4: Solution at $t = 10$ initiated with a Gaussian profile. Comparing the narrow-stencil SBP-SAT method (third row), to the Ignoring method using either a narrow-stencil (second row) and a wide stencil (first row). The left and right columns present the solutions using 101 and 201 grid-points respectively.

The left boundary closure of the diagonal matrix $C_6^{(6)}$ is given by:

$$[0 \ 0 \ 0 \ 0 \ 106.92521670797294276 \ 11.429565737638910841 \ 1 \ \dots].$$

The corresponding right boundary closure is given by a permutation of both rows and columns.

The interior stencil of $M^{(b)}$ at row i is given by ($i = 10 \dots N - 9$):

$$\begin{aligned} m_{i, i-5} &= -\frac{1}{1200} b_{i-3} + \frac{1}{1200} b_{i-2} \\ m_{i, i-4} &= \frac{1}{120} b_{i-2} - \frac{1}{120} b_{i-1} \\ m_{i, i-3} &= -\frac{1}{240} b_{i-2} + \frac{1}{48} b_{i-1} - \frac{1}{45} b_{i-3} - \frac{1}{180} b_i \\ m_{i, i-2} &= \frac{1}{30} b_{i-3} - \frac{13}{60} b_{i-1} + \frac{1}{60} b_{i+1} + \frac{23}{120} b_{i-2} + \frac{1}{8} b_i \\ m_{i, i-1} &= -\frac{1}{80} b_{i-3} - \frac{13}{48} b_{i-2} - \frac{47}{240} b_{i+1} - \frac{1}{240} b_{i+2} - \frac{11}{20} b_{i-1} - \frac{7}{15} b_i \\ m_{i, i} &= \frac{1}{450} b_{i-3} + \frac{13}{150} b_{i-2} + \frac{119}{120} b_{i-1} + \frac{13}{15} b_{i+1} + \frac{7}{150} b_{i+2} + \frac{1}{1800} b_{i+3} + \frac{131}{180} b_i \\ m_{i, i+1} &= -\frac{1}{80} b_{i-2} - \frac{13}{48} b_{i-1} - \frac{47}{240} b_{i+2} - \frac{1}{240} b_{i+3} - \frac{11}{20} b_i - \frac{7}{15} b_{i+1} \\ m_{i, i+2} &= \frac{1}{30} b_{i-1} - \frac{13}{60} b_{i+1} + \frac{1}{60} b_{i+3} + \frac{23}{120} b_i + \frac{1}{8} b_{i+2} \\ m_{i, i+3} &= -\frac{1}{240} b_{i+1} + \frac{1}{48} b_{i+2} - \frac{1}{45} b_i - \frac{1}{180} b_{i+3} \\ m_{i, i+4} &= \frac{1}{120} b_{i+2} - \frac{1}{120} b_{i+3} \\ m_{i, i+5} &= -\frac{1}{1200} b_{i+2} + \frac{1}{1200} b_{i+3} \end{aligned}$$

The left boundary closure of M_a (given by a 9×9 matrix) is given by

$$\begin{aligned}
m_{1,1} &= 0.79126675946955820939 b_1 + 0.29684720906380007429 b_2 + 0.0031855190887964290152 b_3 \\
&\quad + 0.016324040425909519534 b_4 + 0.018279856869297876235 b_5 + 0.076488590391279866843 b_6 \\
m_{1,2} &= -1.0166893393503381444 b_1 - 0.028456273704916113690 b_3 \\
&\quad - 0.041280298383492988198 b_4 - 0.099304230470041228369 b_5 - 0.27892842290602634013 b_6 \\
m_{1,3} &= 0.070756429372437150463 b_1 - 0.18454761060241510503 b_2 - 0.043641631471118923470 b_4 \\
&\quad + 0.21441407223887313279 b_5 + 0.34727028367210028845 b_6 \\
m_{1,4} &= 0.22519915328913532127 b_1 - 0.16627487110970548953 b_2 + 0.027105309616486712977 b_3 \\
&\quad - 0.21064803313780870846 b_5 - 0.14005362655934240416 b_6 \\
m_{1,5} &= -0.052244034642020563167 b_1 + 0.044400639485098762210 b_2 - 0.0010239765473093878745 b_3 \\
&\quad + 0.074034846453161740905 b_4 - 0.0059281241314306605515 b_6 + 0.10402453827138899737 b_5 \\
m_{1,6} &= -0.018288968138771973527 b_1 + 0.0095746331632217580607 b_2 - 0.00081057845305764042779 b_3 \\
&\quad - 0.0073488455877755196984 b_4 - 0.0028672468318208304233 b_5 - 0.020835768843153818676 b_6 \\
m_{1,7} &= 0.0019118885633161709274 b_4 - 0.036178213210074410677 b_5 + 0.034266324646758239749 b_6 \\
m_{1,8} &= 0.013519413163846151226 b_5 - 0.013519413163846151226 b_6 \\
m_{1,9} &= 0.0012401568936609796917 b_6 - 0.0012401568936609796917 b_5 \\
m_{2,2} &= 1.3063321571116676286 b_1 + 0.25420017604573457435 b_3 + 0.10438978280925626095 b_4 \\
&\quad + 0.54759764814820636144 b_5 + 1.0554586309468635698 b_6 \\
m_{2,3} &= -0.090914102699924646049 b_1 + 0.11036113131714764253 b_4 - 1.2040279995862521452 b_5 \\
&\quad - 1.4119275166852918389 b_6 \\
m_{2,4} &= -0.28935573956534316666 b_1 - 0.24213200040645927216 b_3 + 1.2445555514405249075 b_5 \\
&\quad + 0.72477941075349975349 b_6 \\
m_{2,5} &= 0.067127744758037639890 b_1 + 0.0091471926820756301800 b_3 - 0.18721961430038080217 b_4 \\
&\quad - 0.14038341024582559714 b_6 - 0.58346165054822785841 b_5 \\
m_{2,6} &= 0.023499279745900688694 b_1 + 0.0072409053835651813164 b_3 + 0.018583789963916794487 b_4 \\
&\quad - 0.052432560546819092900 b_5 + 0.19323975829294260124 b_6 \\
m_{2,7} &= -0.0048347914064469075906 b_4 + 0.21757451847922370652 b_5 - 0.21273972707277679893 b_6 \\
m_{2,8} &= -0.077457174055292107257 b_5 + 0.077457174055292107257 b_6 \\
m_{2,9} &= -0.0069558971386774566514 b_6 + 0.0069558971386774566514 b_5 \\
m_{3,3} &= 0.0063271611471368738078 b_1 + 0.11473182007158685275 b_2 + 0.11667405542796800075 b_4 \\
&\quad + 2.7042570758920834852 b_5 + 2.1464358133871507134 b_6 \\
m_{3,4} &= 0.020137694138847972466 b_1 + 0.10337179946308864017 b_2 - 2.9542894597368805789 b_5 \\
&\quad - 1.5255086141119696140 b_6 \\
m_{3,5} &= -0.0046717510915754628683 b_1 - 0.027603533656377128278 b_2 - 0.19792902986208699745 b_4 \\
&\quad + 0.73357645900751758204 b_6 + 1.3087034728864726238 b_5 \\
m_{3,6} &= -0.0016354308669218878195 b_1 - 0.0059524752758832596197 b_2 + 0.01964682777442752194 b_4 \\
&\quad + 0.29445166115631844523 b_5 - 0.65846660130947456850 b_6 \\
m_{3,7} &= -0.0051113531893524745496 b_4 - 0.52584603957369764418 b_5 + 0.53095739276305011873 b_6 \\
m_{3,8} &= 0.17793928197257213535 b_5 - 0.17793928197257213535 b_6
\end{aligned}$$

$$\begin{aligned}
m_{3,9} &= 0.015602065249489454152 b_6 - 0.015602065249489454152 b_5 \\
m_{4,4} &= 0.064092997759871869867 b_1 + 0.093136576388046999489 b_2 + 0.23063676246347492291 b_3 \\
&\quad + 3.6623919296010232986 b_5 + 1.8082911165036322918 b_6 + 0.00055555555555555556 b_7 \\
m_{4,5} &= -0.014868958192656041286 b_1 - 0.024870405993901607642 b_2 - 0.0087129289077117541871 b_3 \\
&\quad - 1.6109645175315256576 b_6 - 0.00416666666666666667 b_7 - 1.4249003190038345689 b_5 \\
m_{4,6} &= -0.0052051474298559556576 b_1 - 0.0053630987475285424890 b_2 - 0.0068971427657906095463 b_3 \\
&\quad - 0.80499248194818985658 b_5 + 0.01666666666666666667 b_7 + 1.2293945992864266927 b_6 \\
m_{4,7} &= 0.67614594398793210102 b_5 - 0.68170149954348765658 b_6 - 0.00555555555555555556 b_7 \\
m_{4,8} &= -0.20525046883249159228 b_5 + 0.21358380216582492562 b_6 - 0.00833333333333333333 b_7 \\
m_{4,9} &= -0.017820670963058331298 b_6 + 0.00083333333333333333 b_7 + 0.016987337629724997965 b_5 \\
m_{5,5} &= 0.0034494550959102336252 b_1 + 0.0066411834994278261016 b_2 + 0.00032915450832718628585 b_3 \\
&\quad + 0.33577217075764772000 b_4 + 2.3628974360685559936 b_6 + 0.048323477293104793729 b_7 \\
&\quad + 0.00055555555555555556 b_8 + 0.63338959191282871578 b_5 \\
m_{5,6} &= 0.0012075440723041938061 b_1 + 0.0014321166657521476075 b_2 + 0.00026055826461832559573 b_3 \\
&\quad - 0.033329411132516353908 b_4 - 0.20246057583908584158 b_7 - 0.00416666666666666667 b_8 \\
&\quad - 1.4824154418146444819 b_6 + 0.13715899064776954122 b_5 \\
m_{5,7} &= 0.0086710380841746926251 b_4 + 0.24307726825566136465 b_6 + 0.01666666666666666667 b_8 \\
&\quad + 0.13494086375862876238 b_7 - 0.25335583676513148631 b_5 \\
m_{5,8} &= -0.10575398568559599801 b_6 + 0.014206090827580825082 b_7 + 0.085992339302459617369 b_5 \\
&\quad - 0.00555555555555555556 b_8 \\
m_{5,9} &= 0.0058943160772874548675 b_6 + 0.0099901439597714603961 b_7 - 0.00833333333333333333 b_8 \\
&\quad - 0.0075511267037255819302 b_5 \\
m_{6,6} &= 0.00042272261734493450425 b_1 + 0.00030882419443789644048 b_2 + 0.00020625757066474306202 b_3 \\
&\quad + 0.0033083434042009682567 b_4 + 0.56911889997624958487 b_5 + 0.89317563668967669967 b_7 \\
&\quad + 0.04666666666666666667 b_8 + 0.00055555555555555556 b_9 + 1.2084593155474251732 b_6 \\
m_{6,7} &= -0.00086070442526864133026 b_4 - 0.17024350835350491183 b_5 - 0.19583333333333333333 b_8 \\
&\quad - 0.00416666666666666667 b_9 - 0.62246566552004473067 b_6 - 0.50643012170118171617 b_7 \\
m_{6,8} &= 0.031441424201251809370 b_5 - 0.19015769664365663366 b_7 + 0.01666666666666666667 b_9 \\
&\quad + 0.16704960577573815763 b_6 + 0.12500000000000000000 b_8 \\
m_{6,9} &= 0.010793909172419174918 b_7 + 0.02083333333333333333 b_8 - 0.013959801415215025012 b_6 \\
&\quad - 0.0016351783012546889589 b_5 - 0.00555555555555555556 b_9 \\
m_{7,7} &= 0.00022392237357715991790 b_4 + 0.12602178119583296776 b_5 + 0.89466466943437285361 b_6 \\
&\quad + 0.86666666666666666667 b_8 + 0.04666666666666666667 b_9 + 0.00055555555555555556 b_{10} \\
&\quad + 0.78742296032955035204 b_7 \\
m_{7,8} &= -0.037139096442070555085 b_5 - 0.20643078185674772874 b_6 - 0.19583333333333333333 b_9 \\
&\quad - 0.00416666666666666667 b_{10} - 0.58976345503451504951 b_7 - 0.46666666666666666667 b_8
\end{aligned}$$

$$\begin{aligned}
m_{7,9} &= 0.020372018893214338185 b_6 - 0.216666666666666667 b_8 + 0.016666666666666667 b_{10} \\
&\quad + 0.20160753042529542904 b_7 + 0.125000000000000000 b_9 + 0.0030204506814902327721 b_5 \\
m_{8,8} &= 0.011979461807181236192 b_5 + 0.050400457058697619692 b_6 + 1.0181756366896766997 b_7 \\
&\quad + 0.866666666666666667 b_9 + 0.046666666666666667 b_{10} + 0.000555555555555556 b_{11} \\
&\quad + 0.7277777777777778 b_8 \\
m_{8,9} &= -0.0048475763767907968615 b_6 - 0.27746057583908584158 b_7 - 0.195833333333333333 b_{10} \\
&\quad - 0.004166666666666667 b_{11} - 0.550000000000000000 b_8 - 0.4666666666666667 b_9 \\
&\quad - 0.0010251811174566948874 b_5 \\
m_{9,9} &= 0.00047538878008938292799 b_6 + 0.088323477293104793729 b_7 + 0.9916666666666667 b_8 \\
&\quad + 0.8666666666666667 b_{10} + 0.0466666666666667 b_{11} + 0.0005555555555556 b_{12} \\
&\quad + 0.7277777777777778 b_9 + 0.000090022815694712231457 b_5
\end{aligned}$$

The corresponding right boundary closure is given by replacing $b_i \rightarrow b_{N+1-i}$ for $i = 1..12$ followed by a permutation of both rows and columns.

References

- [1] D. Appelö and N. A. Petersson. A stable finite difference method for the elastic wave equation on complex geometries with free surfaces. *J. Comput. Phys.*, 5:84–107, 2009.
- [2] A. Bamberger, R. Glowinski, and Q.H Tran. A domain decomposition method for the acoustic wave equation with discontinuous coefficients and grid change. *SIAM J. Num. Anal.*, 34(2):603–639, 1997.
- [3] G. Calabrese. Finite differencing second order systems describing black holes. *Physical Review D*, 71:027501, 2005.
- [4] M. H. Carpenter, D. Gottlieb, and S. Abarbanel. Time-stable boundary conditions for finite-difference schemes solving hyperbolic systems: Methodology and application to high-order compact schemes. *J. Comput. Phys.*, 111(2), 1994.
- [5] G. Cohen and P. Joly. Construction and analysis of fourth-order finite difference schemes for the acoustic wave equation in nonhomogeneous media. *SIAM J. Num. Anal.*, 33(4):1266–1302, 1996.
- [6] M. Grote, A. Schneebeli, and D. Schötzau. Discontinuous Galerkin finite element method for the wave equation. *SIAM J. Num. Analysis*, 44:2408–2431, 2006.
- [7] M. Grote, A. Schneebeli, and D. Schötzau. Interior penalty discontinuous galerkin method for maxwell’s equations: Energy norm error estimates. *Journal of Computational and Applied Mathematics*, 204:375–386, 2007.
- [8] B. Gustafsson. The convergence rate for difference approximations to general mixed initial boundary value problems. *SIAM J. Numer. Anal.*, 18(2):179–190, Apr. 1981.
- [9] B. Gustafsson, H.-O. Kreiss, and J. Olinger. *Time dependent problems and difference methods*. John Wiley & Sons, Inc., 1995.
- [10] B. Gustafsson and P. Wahlund. Time compact difference methods for wave propagation in discontinuous media. *SIAM J. Sci. Comput.*, 26:272–293, 2004.
- [11] Ramji Kamakoti and Carlos Pantano. High-order narrow stencil finite-difference approximations of second-order derivatives involving variable coefficients. *SIAM J. Scientific Computing*, 31(6):4222–4243, 2009.

- [12] K. R. Kelly, R. W. Ward, S. Treitel, and R. M. Alford. Synthetic seismograms: A finite difference approach. *Geophysics*, 41:2–27, 1976.
- [13] H.-O. Kreiss, N.A. Petersson, and J. Yström. Difference approximations for the second order wave equation. *SIAM J. Num. Anal.*, 40:1940–1967, 2002.
- [14] S. K. Lele. Compact finite difference schemes with spectral-like resolution. *J. Comput. Phys.*, 103:16–42, 1992.
- [15] K. Mattsson and M. H. Carpenter. Stable and accurate interpolation operators for high-order multi-block finite-difference methods. *SIAM J. Sci Comput.*, 32(4):2298–2320, 2010.
- [16] K. Mattsson, F. Ham, and G. Iaccarino. Stable and accurate wave propagation in discontinuous media. *J. Comput. Phys.*, 227:8753–8767, 2008.
- [17] K. Mattsson and J. Nordström. Summation by parts operators for finite difference approximations of second derivatives. *J. Comput. Phys.*, 199(2):503–540, 2004.
- [18] K. Mattsson, M. Svärd, and J. Nordström. Stable and Accurate Artificial Dissipation. *Journal of Scientific Computing*, 21(1):57–79, August 2004.
- [19] K. Mattsson, M. Svärd, and M. Shoeybi. Stable and accurate schemes for the compressible navier-stokes equations. *J. Comput. Phys.*, 227(4):2293–2316, 2008.
- [20] J. Nordström and M. H. Carpenter. Boundary and interface conditions for high-order finite-difference methods applied to the Euler and Navier-Stokes equations. *J. Comput. Phys.*, 148:341–365, 1999.
- [21] J. Nycander. Tidal generation of internal waves from a periodic array of steep ridges. *J. Fluid Mech.*, 567:415–432, 2006.
- [22] G.R. Shubin and J.B. Bell. A modified equation approach to constructing fourth order methods for acoustic wave propagation. *SIAM J. Sci. Stat. Comput.*, 8(2):135–151, 1987.
- [23] M. Svärd. On coordinate transformation for summation-by-parts operators. *Journal of Scientific Computing*, 20(1), 2004.

- [24] M. Svärd, M. H. Carpenter, and J. Nordström. A stable high-order finite difference scheme for the compressible Navier–Stokes equations, far-field boundary conditions. *J. Comput. Physics*, 225:1020–1038, February 2008.
- [25] M. Svärd, M. H. Carpenter, and J. Nordström. A stable high-order finite difference scheme for the compressible Navier–Stokes equations, no-slip wall boundary conditions. *J. Comput. Physics*, 227:4805–4824, May 2008.
- [26] M. Svärd, K. Mattsson, and J. Nordström. Steady-state computations using summation-by-parts operators. *Journal of Scientific Computing*, 24(1):79–95, July 2005.
- [27] M. Svärd and J. Nordström. On the order of accuracy for difference approximations of initial-boundary value problems. *J. Comput. Physics*, 218:333–352, October 2006.
- [28] B. Szilagyil, H.-O. Kreiss, and J.W Winicour. Modeling the black hole excision problem. *Physical Review D*, 71:104035, 2005.
- [29] J. Virieux. Sh-wave propagation in heterogeneous media: Velocity-stress finite-difference method. *Geophysics*, 49:1933–1957, 1984.
- [30] J. Virieux. P-sv wave propagation in heterogeneous media: Velocity-stress finite-difference method. *Geophysics*, 51:889–901, 1986.
- [31] K.S. Yee. Numerical solution of initial boundary value problems involving maxwells equations in isotropic media. *IEEE Trans. Antennas Propag.*, 14:302–307, 1966.